Time-dependent plasticization behavior of polyimide membranes at supercritical conditions

Journal of Membrane Science 635 (2021) 119512

Contents lists available at ScienceDirect

Journal of Membrane Science

journal homepage: www.elsevier.com/locate/memsci

Time-dependent plasticization behavior of polyimide membranes at supercritical conditions

Menno Houben, Machiel van Essen, Kitty Nijmeijer, Zandrie Borneman *

Membrane Materials and Processes, Department of Chemical Engineering and Chemistry, Eindhoven University of Technology, P.O. Box 513, 5600, MB, Eindhoven, the Netherlands

ARTICLE INFO

Keywords:
Supercritical CO_2
Time-dependency
CO_2 plasticization
Polyimide membrane

ABSTRACT

The time-dependent CO_2-induced plasticization behavior of glassy Matrimid® 5218 polymer membranes at supercritical conditions up to 120 bar was investigated. Glassy polyimide membranes were conditioned with both gaseous CO_2 and liquid-like sc-CO_2. The plasticization behavior during permeation and sorption was correlated with the intrinsic membrane properties and the CO_2 fluid properties. In the gaseous region the CO_2 concentration increased slightly over time, while in the liquid-like sc-CO_2 region the CO_2 concentration remained constant over time and showed no hysteresis, indicating an induced glass transition. Contrary to the CO_2 sorption the CO_2 permeability showed more pronounced time-dependent behavior which increases with feed pressure because of polymer membrane plasticization. Despite the strong time-dependency, the CO_2 permeability was independent of the feed pressure in the liquid-like sc-CO_2 region. This difference in time-dependent behavior between sorption and permeation is due to the presence of a concentration gradient during permeation experiments. In addition, the permeability showed significant hysteresis. Exposure to liquid-like sc-CO_2 resulted in a highly plasticized membrane and changed the permeation behavior at all subsequent feed pressures, due to slow polymer chain relaxation rates. Clearly, these relationships proof that the permeation history is a critical aspect for time-dependent plasticization phenomena at high CO_2 pressures.

1. Introduction

Glassy dense polymer membranes are commonly used in CO_2 gas separations. It is well known that high concentrations of CO_2 induce plasticization phenomena in these glassy polymer membranes [1–6]. The polymer matrix swells due to high CO_2 sorption increasing the polymer free volume and chain mobility. Consequently, the diffusivity of the permeating species increases resulting in significantly higher permeabilities. The diffusivity of especially the slower permeating species benefits the most from this increase in free volume. Therefore, plasticization generally decreases the membrane selectivity [7–9]. The extent of plasticization is closely correlated with the CO_2 concentration inside the polymer matrix and the CO_2 concentration in the polymer matrix scales with the CO_2 partial pressure [10]. Therefore, glassy polymers especially suffer from severe plasticization in high pressure applications, *e.g.* CO_2/CH_4 separation [9]. Additionally, at pressures and temperatures above the critical point (74 bar, 31 °C) CO_2 is in the supercritical state [11]. Supercritical carbon dioxide (sc-CO_2) has significantly different properties compared to gaseous CO_2, most notably its density and viscosity (Fig. 1) [11]. Till now, the effect of sc-CO_2 and its fluid properties on the membrane performance and the plasticization behavior is not much studied, while it does have a large impact on the performance in high pressure applications (*e.g.* sc-CO_2 extractions or enhanced methane recovery) [12–17].

Previous work shows that the CO_2 density is the most important fluid property influencing plasticization phenomena in polymer membranes and thus the CO_2 permeability behavior at supercritical conditions [12,18]. Although supercritical CO_2 is often described having a liquid-like density, even within the supercritical region, a distinction can be made between a less dense gaseous-like region and a denser liquid-like region [19,20]. It is this quasi-phase transition from gaseous-like to liquid-like sc-CO_2 in the supercritical region that causes a steep increase in CO_2 density. Based on this, Shamu et al. [18] concluded that not the phase transition from gaseous to supercritical CO_2, but the quasi-phase transition within the supercritical region is the crucial transition influencing the CO_2 permeability behavior in polymer membranes.

In our previous work we showed that the CO_2 concentration profile in a glassy polyimide matrix follows the CO_2 density profile and

* Corresponding author.
E-mail address: z.borneman@tue.nl (Z. Borneman).

https://doi.org/10.1016/j.memsci.2021.119512
Received 23 March 2021; Received in revised form 31 May 2021; Accepted 3 June 2021
Available online 10 June 2021

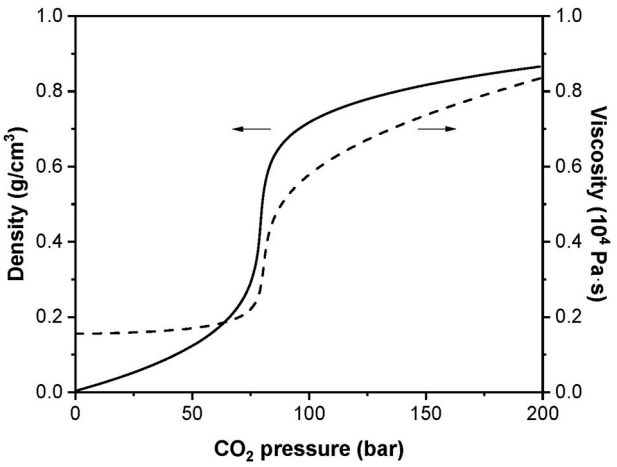

Fig. 1. Density and viscosity of CO_2 as a function of pressure at 35 °C. Data is obtained from the database of the National Institute of Standards and Technology [11]. The quasi-phase transition from gaseous-like to liquid-like sc-CO_2 occurs at 80 bar.

determines the extent of plasticization [12]. After the quasi-phase transition to liquid-like sc-CO_2, the CO_2 density and thus the CO_2 concentration in the polymer matrix started to level off. Accordingly, it was hypothesized that the swelling stresses in the liquid-like sc-CO_2 regime remain relatively constant. With that, also the extent of plasticization was indirectly shown not to increase further when increasing the feed pressure in this liquid-like sc-CO_2 regime. However, the experimental times in our previous work were relatively short, while plasticization has a large time-dependency [5,6,21,22]. Above the plasticization pressure the polymer matrix swells over time. This is because of the large swelling stresses imposed on the membrane upon high CO_2 sorption, resulting in a continuous increase in permeability. The magnitude of this increase in permeability is dependent on the feed pressure and the permeation history of the membrane film [6]. At lower feed pressures the swelling stresses are smaller than at higher feed pressures. Therefore, the morphological state of the membrane film can change if the membrane has already been in contact with CO_2, even at lower pressures. At supercritical conditions, thus at high pressures, these time-dependent plasticization characteristics can largely influence the membrane performance. This is undesirable when stable and predictable membrane separation performance is required. Therefore, understanding plasticization phenomena at a molecular level and comprehending how key parameters play a role in the effects of plasticization is vital when developing new plasticization resistant membranes.

This study thus focusses on the time-dependent plasticization behavior of glassy polymer membranes at supercritical CO_2 conditions. Glassy polyimide membranes are conditioned with both gaseous CO_2 (low density) and liquid-like sc-CO_2 (high density) and the observed plasticization behavior is correlated with the CO_2 fluid properties and the permeation behavior. To study the time-dependency of the plasticization phenomena at supercritical CO_2 conditions the CO_2 permeability and sorption were measured as a function of time at different pressures in the gaseous CO_2 and the liquid-like sc-CO_2 region. The permeation and sorption behavior are compared to discuss the plasticization behavior on a molecular level. To further assess network dilation and relaxation kinetics at these conditions, N_2 permeance decay measurements are performed after CO_2 conditioning. Finally, the influence of the permeation history at low CO_2 pressures on the CO_2 permeability at high CO_2 pressures is investigated.

2. Experimental

2.1. Materials

Matrimid® 5218 (Matrimid), polyimide, was kindly provided by Huntsman Advance Materials (Europe). N, N-Dimethylformamide (DMF, ≥ 99.9%), was obtained from Biosolve, The Netherlands and was used without further purification. Pure gasses (CO_2, He and N_2) were purchased from Linde Gas with a purity of ≥99.995% and were used as received.

2.2. Membrane preparation

Dense Matrimid films were made by casting a 20 wt% Matrimid solution in DMF on a glass substrate using a 0.5 mm doctor blade. Prior to casting, the solution was filtered to remove any remaining solid particles using a 5 μm aluminum filter. The Matrimid films were dried following the same protocol as in our previous work [3]. First, the cast films were solidified at room temperature in a nitrogen atmosphere for 48 h. Subsequently, residual solvent in the membrane films was removed in a nitrogen oven at 80 °C for 24 h, 120 °C for 24 h and 150 °C for 48 h. The thickness of the resulting Matrimid films was measured using an IP65 Coolant Proof digital Micrometer from Mitutoyo and was found to be between 40 and 50 μm.

2.3. High pressure gas sorption

Time-dependent gas sorption isotherms of CO_2 in dense Matrimid films were determined gravimetrically using a magnetic suspension balance (MSB, Rubotherm series IsoSORP® sorption instrument). CO_2 was pressurized into the supercritical state using a high-pressure syringe pump (Teledyne ISCO 260D syringe pump). The temperature was kept constant at 35 °C for all experiments. Before each measurement the sample was degassed for at least 12 h. Subsequently, the time-dependency of the CO_2 sorption was measured at pressures of 20, 40 and 60 bar in the gaseous CO_2 state and 85, 100 and 120 bar in the liquid-like sc-CO_2 state. For each conditioning pressure, the measurement consisted of a pressurization cycle where the pressure was gradually increased to the desired pressure with incremental pressure steps using a 3 h time interval, followed by three days at isobaric conditions. For all sorption measurements pristine membranes were taken to exclude any history effects. The mass uptake of CO_2 in the dense Matrimid films was corrected for swelling dependent buoyancy based on the initial sample weight and volume according to equation (1).

$$m_{CO_2} = m_t + [V_s \cdot (1 + \gamma_{sw})] \cdot \rho_{CO_2} - m_0 \quad (1)$$

In equation (1) m_{CO_2} (g) is the swelling dependent buoyancy corrected mass uptake of CO_2 in the polymer, m_t (g) is the measured mass of the sample at time t, V_s (cm^3) is the volume of the sample in the initial state, γ_{sw} (−) is the pressure and temperature dependent volumetric swelling coefficient, ρ_{CO_2} (g/cm^3) is the density of the surrounding CO_2 at the measured pressure and temperature (determined by the MSB) and m_0 (g) is the initial mass of the sample measured at vacuum. Volumetric swelling values per pressure step were calculated by the extrapolation of volumetric swelling values obtained from literature for polyimides comparable to Matrimid, as described in more detail in our previous work [4,12]. Although in some cases this may introduce small discrepancies between the calculated swelling values and the actual swelling values, this approach provides within the existing possibilities the most accurate swelling values.

2.4. High pressure gas permeation

The high-pressure time-dependent permeation properties of dense Matrimid films were determined using a custom build high-pressure

permeation setup. The membrane under investigation was placed into a stainless steel cell with an effective permeation area of 78.8 cm^2 (membrane cell is described in detail by Shamu et al. [18]). Additionally, a Whatman® filter paper (Grade 50 with pore size of 2.7 μm) supported the membrane to prevent possible pressure induced punctures. The temperature during measurements was controlled with a HAAKE W19 water bath with D1 heater and all permeation measurements were performed at a temperature of 35 °C. The desired pressure was applied to the feed side of the membrane using a high-pressure Teledyne ISCO-pump 260D syringe pump, while keeping the permeate side at atmospheric pressure. Permeation flowrates were recorded using a bubble flowmeter and the corresponding permeability coefficients were calculated using equation (2).

$$P_i = \frac{J_i \cdot l}{\Delta f_i} \quad (2)$$

Here P_i (cm^3 (STP) cm/(cm^2 s cmHg)) is the permeability coefficient, J_i (cm^3 (STP)/(cm^2 s)) is the flux, l (cm) is the thickness of the membrane and Δf_i (cmHg) is the fugacity difference of the feed and permeate. At high CO_2 pressures, the non-ideal behavior of CO_2 becomes increasingly more important. Therefore, fugacities should be used as a driving force for the calculation of the permeabilities instead of absolute partial pressures. The fugacity is the effective partial pressure, *i.e.* the partial pressure corrected for non-ideal gas behavior. Fugacities were calculated using the Soave-Redlich-Kwong equation of state for CO_2 at 35 °C for pressures up to 120 bar and are shown in Fig. 2 [23]. Reported permeability values are averages of triplicate measurements. Each new membrane was first evaluated for its intrinsic N_2 permeability at 20 bar to ensure a defect-free membrane.

Time-dependent CO_2 permeabilities were measured at pressures of 20, 40 and 60 bar in the gaseous CO_2 state and 85, 100 and 120 bar in the liquid-like sc-CO_2 state. For each conditioning pressure the measurement consisted of a pressurization cycle followed by three days at isobaric conditions. During the pressurization cycle the pressure was gradually increased to the desired pressure with the following pressure increments 20, 40, 60, 70, 80, 100 and 120 bar using a 1 h time interval. At the final pressure step the time-dependent CO_2 permeability was measured for three days at constant pressure. For each CO_2 conditioning measurement pristine membranes were taken to exclude history effects. After CO_2 conditioning the N_2 permeability decay at 20 bar was measured over time period of five days to identify the effects of CO_2 conditioning on the elastic and plastic component of network dilation.

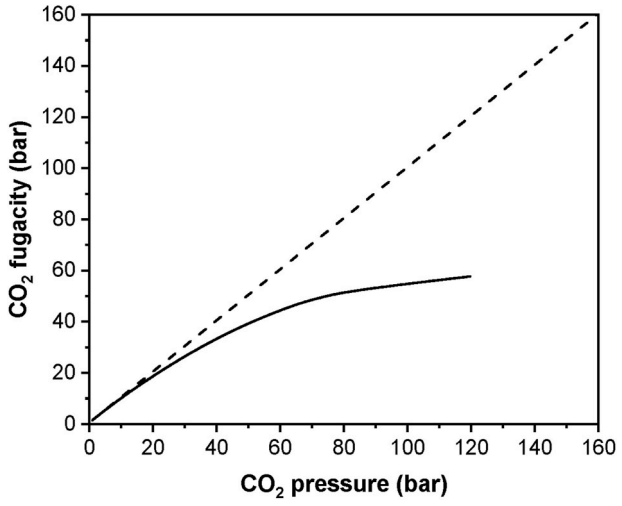

Fig. 2. CO_2 fugacity calculated using the Soave-Redlich-Kwong equation of state as a function of the CO_2 pressure at 35 °C (solid black line) [23]. The dashed line represent unity. The quasi-phase transition from gaseous-like to liquid-like sc-CO_2 occurs at 80 bar.

Hysteresis measurements were performed on pristine membranes, which consists of a pressurization, depressurization and a repressurization cycle. Initially, the pressure was gradually increased from 20 to 120 bar using the same pressure increments as for the time-dependent measurements (20, 40, 60, 85, 100 and 120 bar) with a time interval of 24 h at each pressure stage. At each pressure stage the CO_2 permeability was measured as a function of the experimental time. Subsequently, after the final pressure was reached the pressure was gradually decreased back to 20 bar using the same protocol. The protocol for the repressurization cycle was identical as for the pressurization cycle.

To study the influence of the permeation history of the membrane, membranes were exposed to CO_2 for different conditioning times. The pressure was incrementally increased from 20 to 120 bar using either 1 h or 24 h conditioning time for each preceding pressure step (Fig. 3). The reported permeability values were taken after 24 h of permeation at the respective pressure for all membranes. Therefore, for the series using 1 h of conditioning time multiple new membranes were used to ensure that these membranes all have a permeation history of 1 h at all previous pressures. This way the difference in permeability was only caused by the difference in permeation history.

3. Results and discussion

3.1. High-pressure CO_2 sorption

The sorption and desorption isotherms of CO_2 for Matrimid are shown in Fig. 4. The CO_2 sorption shows the non-linear sorption behavior as a function of pressure typical for glassy polymers [24,25]. In the gaseous CO_2 phase (open symbols) the CO_2 concentration increases with increasing feed pressure and can be well described with the dual-mode sorption model [26–28]. The critical CO_2 concentration of ~38 cm^3(STP)/cm^3, which corresponds to the plasticization pressure, is already reached at around 10 bar [1]. Thus, the effects of plasticization should be clearly visible at relatively low pressures. The extent of plasticization is dependent on the CO_2 concentration in the polymer matrix, and thus becomes more severe as the pressure increases in the gaseous CO_2 phase [10]. The phase transition from gaseous CO_2 to liquid-like sc-CO_2 at 80 bar is clearly reflected in the sorption behavior, indicated by the transition from the open symbols to the solid symbols in Fig. 4 [12]. Near the phase transition pressure (80 bar) the CO_2 density changes significantly with small changes in pressure, resulting in a slight jump in CO_2 concentration when entering the liquid-like sc-CO_2 region. After the phase transition the trend of the CO_2 concentration with increasing pressure closely resembles the trend of the CO_2 density, and both the CO_2 concentration and density start to level off [12,18,29]. Next to that, the driving force (CO_2 fugacity) also starts to level off in the liquid-like sc-CO_2 region (Fig. 2). Thus, the changing CO_2 properties ensures that the CO_2 concentration levels off at liquid-like sc-CO_2 conditions. In the liquid-like sc-CO_2 region the sorption distinctly deviates from the sorption predicted by the dual-mode sorption model. Therefore, the sorption in this liquid-like sc-CO_2 region cannot be described using this model. The CO_2 concentration in the liquid-like sc-CO_2 region reaches a plateau value, resulting in relatively constant swelling stresses in the polymer matrix with increasing pressure [12]. Based on this, we hypothesize that the extent of plasticization also remains relatively constant with increasing CO_2 pressures.

For the desorption isotherm large hysteresis is observed in the gaseous CO_2 region. This large hysteresis reflects slow chain relaxations after plasticization, which is commonly observed for glassy polymers [4]. The dual-mode sorption parameters for both sorption and desorption in the gaseous CO_2 phase are shown in Table 1 [27,28]. Since the dual-mode sorption model cannot describe the sorption in the liquid-like sc-CO_2, only the gaseous phase is considered for the calculation of the dual-mode sorption parameters [30–32]. The dual mode sorption parameters during sorption are comparable to the parameters found in literature [33,34]. When plotting, based on the dual-mode parameters,

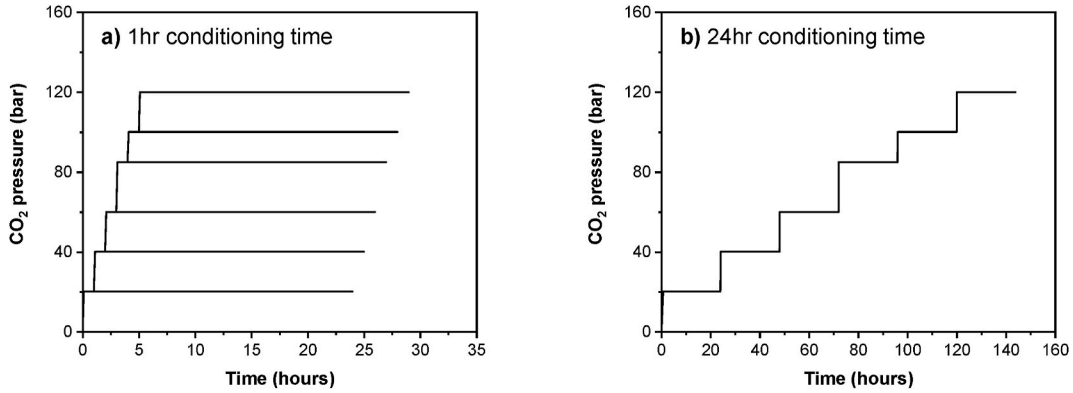

Fig. 3. CO_2 pressure as a function of the experimental time for the membranes with **a)** 1 h conditioning time at preceding pressures and with **b)** 24 h conditioning time at preceding pressures. For the membranes with 1 h conditioning time at preceding pressures each curve represents a pristine membrane.

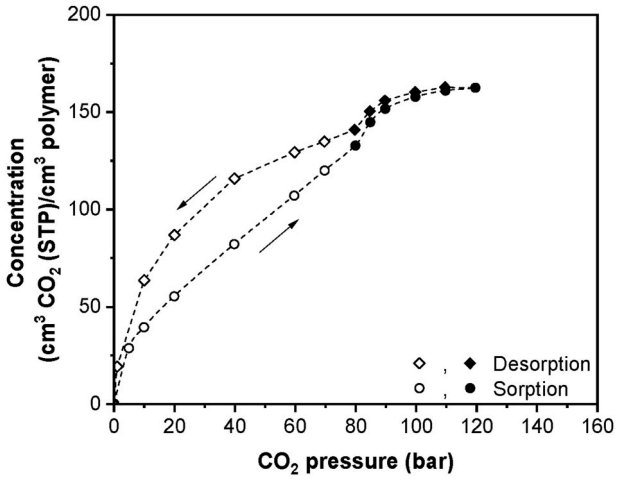

Fig. 4. CO_2 sorption isotherm in Matrimid at 35 °C in a pressurization/depressurization cycle. Values are obtained after 3 h of sorption. The open symbols represent the gaseous CO_2 phase, whereas the closed symbols represent the liquid-like sc-CO_2 phase.

Table 1
Dual mode sorption parameters in the gaseous CO_2 regime for Matrimid during sorption and desorption.

CO_2 sorption mode	C'_H [cm^3(STP)/cm^3]	b [1/bar]	k_D [cm^3(STP)/cm^3·bar]
Sorption	34.57 ± 0.45	0.37 ± 0.02	1.24 ± 0.01
Desorption	107.80 ± 15.30	0.13 ± 0.04	0.55 ± 0.16

the CO_2 sorption isotherms almost coincide. There is a large difference between the parameters during sorption and desorption. At high CO_2 pressures the membrane is highly plasticized, resulting in a highly swollen structure. Decreasing the CO_2 pressure leaves an excess free volume in the polymer matrix, resulting in a considerably larger Langmuir parameter C'_H, which correlates to the amount of non-equilibrium excess free volume present in the polymer matrix [28]. At the same time the Henry's sorption parameter, k_D, is reduced. This shows that after exposure to high pressure CO_2, sorption predominantly takes place in the additional excess free volume created by plasticization.

In contrast to the gaseous CO_2 phase, sorption hysteresis almost completely disappears after the phase transition to liquid-like sc-CO_2. This absence of hysteresis in this region indicates that the high CO_2 sorption induces a glass transition in the polymer matrix [4,35]. Many studies proved that the glass transition temperature (T_g) of the polymer-CO_2 mixture can drop significantly at high CO_2 concentrations [36–41]. Matrimid has a T_g of approximately 328 °C at atmospheric conditions, while the sorption measurements are performed at 35 °C [9]. Therefore, the T_g of the Matrimid-CO_2 mixture needs to drop by almost 300 °C to induce a glass transition at the measurement conditions. In the work of Wessling et al. [38] the T_g of a polyimide that was saturated with CO_2 at 50 bar was experimentally determined by foaming experiments. They observed a considerable drop in T_g from 312 °C to 114 °C, which clearly shows that the strong CO_2-induced plasticization effect significantly lowers the T_g. Therefore, when the CO_2 concentration is even higher at the very high pressures used in this work, a further reduction in T_g of the polyimide-CO_2 mixture, even below the experimental temperature, is very likely. Although high hydrostatic pressures can slightly compress the polymer matrix and marginally increase the T_g of the polymer, this effect is insignificant compared to the effect of plasticization in the used pressure range [36]. Thus, based on the large T_g depression with increasing CO_2 concentration as observed by Wessling et al. [38] and Krause et al. [37], and the results observed in this work, it is highly likely that a glass transition is induced in Matrimid at liquid-like sc-CO_2 conditions.

Plasticization not only has a concentration dependency, but also a time dependency [4,6,21,42]. In Fig. 5 the CO_2 sorption kinetics are shown as a function of the logarithm of time for different pressures in the gaseous CO_2 region (5–60 bar) and in the liquid-like sc-CO_2 region (85–120 bar). The first few minutes of sorption are disregarded due to instabilities in the measured balance weight upon pressurization of the of sorption balance. At higher pressures these instabilities become more pronounced, as small changes in pressure have a large influence on the

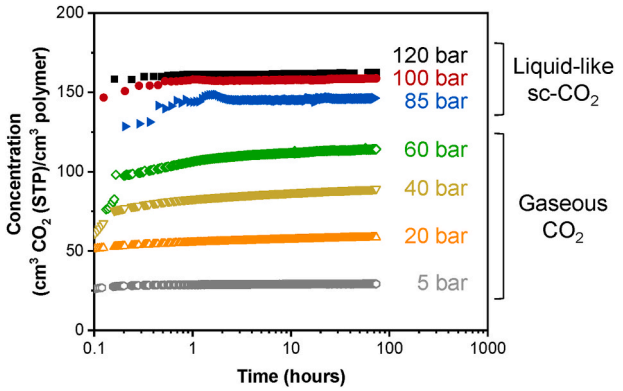

Fig. 5. CO_2 sorption isotherm in Matrimid at 35 °C as a function of the experimental time for different pressures. The open symbols represent the gaseous CO_2 phase whereas the closed symbols represent the liquid-like sc-CO_2 phase.

CO_2 density, especially near the phase transition to liquid-like sc-CO_2 at 80 bar.

In the gaseous CO_2 region, after the initial concentration buildup the CO_2 concentration in the polymer matrix remains constant over time at a pressure of 5 bar, which is expected as the magnitude of plasticization below the plasticization pressure (~10 bar for Matrimid) is very small [3,43]. When increasing the pressure above this plasticization pressure in the gaseous CO_2 region, the CO_2 concentration increases slightly over time. This additional increase in CO_2 concentration over time is caused by the creation of extra free volume due to plasticization of the polymer matrix, which becomes more pronounced at higher pressures. Therefore, also in the gaseous CO_2 state the time-dependent increase in CO_2 concentration is more pronounced at higher pressures. Contrary to the gaseous CO_2 state different time-dependent behavior is observed when the CO_2 pressure is increased into the liquid-like sc-CO_2 region. Interestingly, in this liquid-like sc-CO_2 region the CO_2 concentration remains constant as a function of the experimental time, indicating that the kinetics of plasticization are faster when CO_2 is supplied in the liquid-like sc-CO_2 phase. The fast plasticization kinetics and constant CO_2 concentrations together with the absence of hysteresis in the liquid-like sc-CO_2 region further substantiates that indeed the high sorption of CO_2 induces a glass transition, and the polymer membrane enters its rubbery state. Typically, rubbery polymer membranes do not show any hysteresis phenomena as non-equilibrium excess free volume is absent in rubbery polymers [18,44,45]. Furthermore, rubbery polymers are generally much less affected by plasticization effects and therefore have no significant time-dependent sorption behavior [10,18].

3.2. Time-dependent CO_2 permeability behavior

Fig. 6 shows the CO_2 permeability as a function of time for different pressures in the gaseous CO_2 region (open symbols) and in the liquid-like sc-CO_2 region (closed symbols). In the gaseous CO_2 region, the CO_2 permeabilities show time-dependent permeation behavior at all measured CO_2 conditioning pressures. The plasticization pressure of Matrimid is around 10 bar, therefore all CO_2 permeabilities are measured above the plasticization pressure of Matrimid [1,3]. With increasing CO_2 feed pressure, the CO_2 concentration in the polymer matrix increases, resulting in a more swollen membrane. The CO_2 permeability increases by a factor 1.5 at 20 bar to even a factor 16 at 120 bar, illustrating the power of plasticization phenomena at high pressures. Above the plasticization pressure the measured permeabilities are non-equilibrium values, as they increase in time due to the non-equilibrium state of the glassy polymer [2,6]. These time-dependent characteristics originate from large swelling stresses imposed by high CO_2 sorption. As a result, the polymer matrix swells over time increasing its free volume and therefore increasing the CO_2 permeability over time as well. The CO_2 permeability increases significantly in the first few hours due to the build-up of the concentration profile and the corresponding swelling of the membrane. Subsequently, the CO_2 permeability keeps increasing over time, but at a considerable slower rate, which is displayed by the lower slope of the permeability curves at longer experimental times.

The slopes of the permeability curves, calculated between 50 and 75 h, are shown in Fig. 7. The swelling stresses, which are determined by the CO_2 concentration in the membrane, are larger at higher pressures than at lower pressures. Therefore, increasing the pressure in the gaseous CO_2 region (20–60 bar) results in a larger time-dependent permeability increase, which is illustrated by the exponentially increasing slopes in Fig. 7.

At 35 °C the phase transition to liquid-like sc-CO_2 occurs at 80 bar [11,19]. After the phase transition to liquid-like sc-CO_2 the permeation characteristics are independent of the sc-CO_2 pressure. In this region the CO_2 permeability curves overlap and show the exact same behavior. This behavior is correlated to the CO_2 sorption and the CO_2 density, which level off after the phase transition occurs (Figs. 1 and 4). Because the CO_2 sorption levels off, the swelling stresses in the membrane do not increase further at higher pressures in the liquid-like sc-CO_2 region. This means that in this region the swelling of the membrane, and thus the extent of plasticization, is independent of the feed pressure. This behavior is also observed in the time-dependent increase of the CO_2 permeability, as the slopes of the permeability curves are similar. Accordingly, the extent of plasticization remains constant with increasing pressure in the liquid-like sc-CO_2 region. Interestingly, the slope of the permeability curves in the liquid-like sc-CO_2 region is similar to the slope of the permeability curve at 60 bar in the gaseous CO_2 region, while the absolute CO_2 permeabilities differ significantly. This suggests that the swelling rate at 60 bar and that at pressures in the liquid-like sc-CO_2 is comparable, while the polymer matrix is more swollen in the liquid-like sc-CO_2 region. Even though the extent of plasticization does not increase with increasing pressure in the liquid-like sc-CO_2 region, the polymer matrix still plasticizes, as the CO_2 permeabilities keep increasing over time. This permeation behavior is

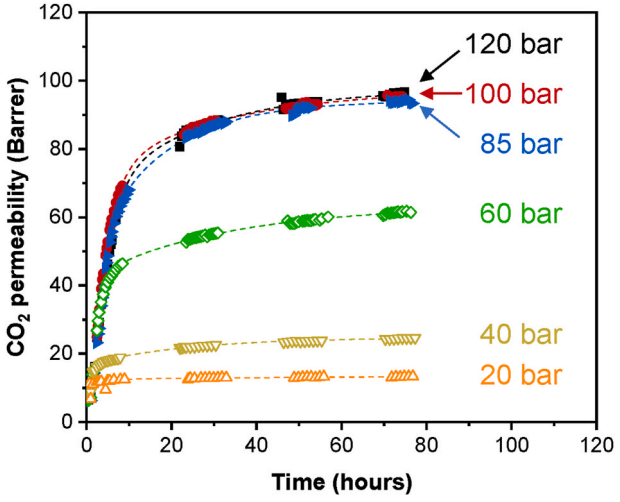

Fig. 6. Time-dependent CO_2 permeability (based on CO_2 fugacity) of Matrimid at 35 °C as a function of the CO_2 conditioning time for different pressures. The open symbols represent the gaseous CO_2 phase whereas the closed symbols represent the liquid-like sc-CO_2 phase.

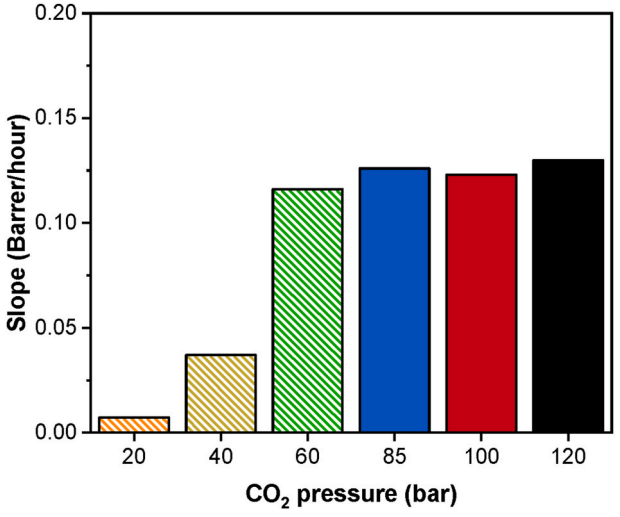

Fig. 7. Slopes of the time-dependent CO_2 permeability curves at different pressures for Matrimid membranes at 35 °C. The slopes of the CO_2 permeability curves are calculated in the experimental time interval 50–75 h. The patterned bars represent the gaseous CO_2 phase whereas the solid bars represent the liquid-like sc-CO_2 phase.

inconsistent with the observed CO_2 sorption behavior (Fig. 5). The CO_2 sorption shows no time-dependent behavior in the liquid-like sc-CO_2 region, which substantiates that the high CO_2 concentrations induce a glass transition in the polymer matrix [4,35]. If a similar glass transition would be induced during permeation measurements than the CO_2 permeability would become time-independent, as rubbery membranes are significantly less affected by plasticization phenomena [10,18]. This difference in observed behavior between permeation and sorption experiments is related to the CO_2 concentration in the polymer matrix [21]. During sorption all sides of the membrane are exposed to high pressure CO_2, which results in a uniform CO_2 concentration in the membrane at steady-state conditions. On the other hand, during permeation only the feed side of the membrane is exposed to high pressure CO_2, while the permeate side is at atmospheric conditions. This results in a CO_2 concentration gradient over the thickness of the membrane, where the CO_2 concentration decreases from the feed to the permeate side, as schematically shown in Fig. 8. Due to this concentration gradient, the CO_2 concentration will not be high enough to surpass the glass transition temperature over the entire thickness of the membrane. Only in a small part of the membrane, the part that faces the feed side, the T_g drops sufficiently to end up in the rubbery phase. Therefore, the membrane primarily shows glassy behavior, which results in the increasing CO_2 permeabilities over time in the liquid-like sc-CO_2 region.

The phase transition from gaseous to liquid-like sc-CO_2 not only causes a steep increase in CO_2 density, but also a steep increase in CO_2 viscosity (Fig. 1). The CO_2 density is a thermodynamic parameter and mostly influences the CO_2 sorption, while CO_2 viscosity is a kinetic parameter, that influences the CO_2 diffusivity [18,46,47]. Shamu et al. [18] observed a decline in CO_2 permeability and diffusion coefficient for rubbery PDMS membranes in the liquid-like sc-CO_2 region due to the increased viscosity of CO_2 at liquid-like conditions. However, for glassy Matrimid membranes the CO_2 sorption remains constant, while the CO_2 permeabilities are independent of the feed pressure and keep increasing over time in the liquid-like sc-CO_2 region. As a consequence, the diffusion coefficient and the permeability change proportionally to each other even in liquid-like conditions due to strong plasticization, as shown in our previous work [12]. This shows that the effect of plasticization in these glassy polymer membranes dominates the effect of the increased viscosity on the CO_2 permeability at liquid-like conditions as seen for rubbery membranes.

3.3. N_2 permeability decay in time

Conditioning of the glassy polymer matrix at high pressure CO_2 results in increasing diffusion coefficients for all permeating species due to plasticization phenomena [1,8]. To further asses these network dilation effects, the N_2 permeability decay in time is measured immediately after exposure to high pressure CO_2. Fig. 9 shows the N_2 permeability decay in time for the different CO_2 conditioning pressures. The measured N_2 permeability after CO_2 exposure is normalized to the initial N_2 permeability that is determined before the membrane has been in contact with CO_2. Clearly, the conditioning of the membrane with CO_2 results in significant plasticization of the polymer matrix as the N_2 permeability is more than 2 times higher at 20 bar and more than 10 times higher at 120 bar than the initial N_2 permeability. The N_2 permeability decreases considerably during the first 25 h, which corresponds to the elastic part of plasticization. Subsequently, the N_2 permeability decreases slowly over time as relaxation of the plasticized polymer matrix occurs [48,49].

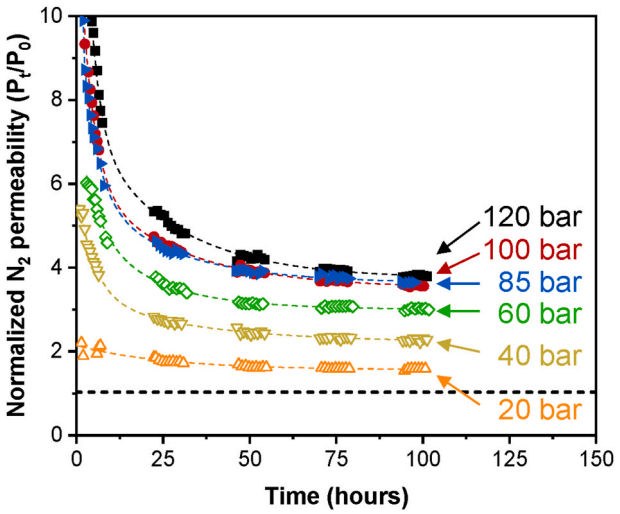

Fig. 9. N_2 permeability decay of Matrimid measured at 20 bar N_2 pressure and 35 °C after different CO_2 conditioning pressures. The N_2 permeability after CO_2 exposure is normalized to the N_2 permeability that is determined before the membrane has been in contact with CO_2. The black dashed line corresponds to a value of 1. The open symbols represent the conditioning of the membrane in the gaseous CO_2 phase whereas the closed symbols represent conditioning of the membrane in the liquid-like sc-CO_2 phase.

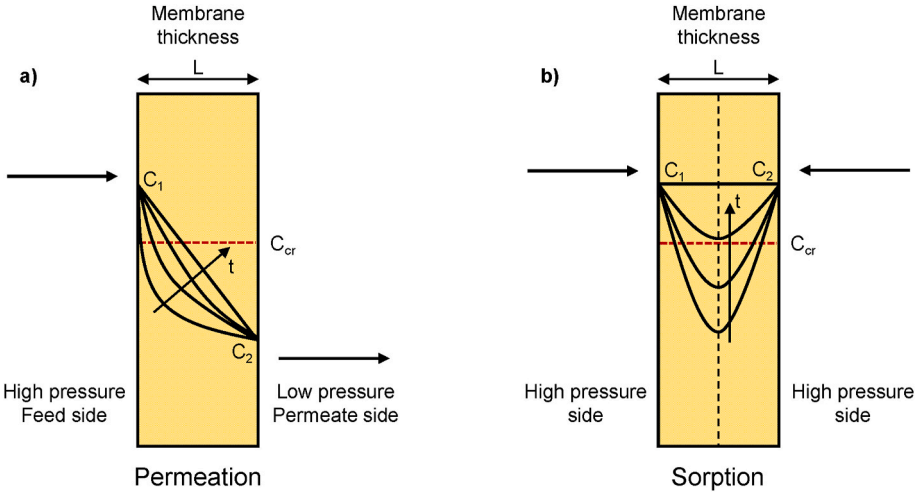

Fig. 8. Authors impression of the concentration profile with increasing time under **a)** permeation and **b)** sorption conditions. The critical CO_2 concentration, C_{cr}, is required to induce a glass transition in the membrane.

However, the polymer chains are unable to relax back to their initial state within the measured time interval (~100 h), indicating permanent network dilation. Over time the polymer matrix keeps relaxing to a denser configuration due to physical aging. Moreover, this process usually occurs over long timescales (months to years) for thick films, especially at temperatures far below the T_g of Matrimid [50–53].

At higher CO_2 conditioning pressures, the N_2 permeability increases indicating a higher degree of plasticization, and thus swelling, of the polymer matrix. Similar behavior is observed for the N_2 permeability decay as for the CO_2 permeability when the membrane is conditioned at pressures in the liquid-like sc-CO_2 region. The N_2 permeability decay follows the same course after being exposed to 85, 100 and 120 bar CO_2, showing that the level of swelling and thus the extent of plasticization is independent of the CO_2 conditioning pressure in the liquid-like supercritical region.

The slopes of the N_2 permeability decay curves provide more information about the relaxation rate of the polymer matrix after CO_2 exposure. The slopes of these curves are shown in Fig. 10 and are calculated in the time interval 50–75 h. The N_2 permeability decreases more rapidly at higher CO_2 conditioning pressures, implying that the polymer matrix has faster chain relaxation after being exposed to higher swelling stresses. Because the N_2 permeability curves of the membranes that were exposed to liquid-like sc-CO_2 are similar, the slopes of these curves are also comparable. This confirms that the relaxation rate of the polymer chains is related the level of swelling, and thus the swelling stresses, of the polymer matrix. Overall, the slopes of the N_2 permeability decay curves show similar behavior to the slopes of the CO_2 permeability curves. However, the slopes of the CO_2 permeability curves correspond to the swelling rate of the polymer matrix during CO_2 exposure, while the slopes of the N_2 permeability correspond to the relaxation of the polymer chains succeeding swelling. The slope of the CO_2 permeability curve at 60 bar is similar to the slopes of the CO_2 permeability curves in the liquid-like sc-CO_2 region (Fig. 7), while this is not the case the slopes of the N_2 permeability curves. This shows that at 60 bar CO_2 pressure the swelling rate of the polymer matrix is similar to the swelling rate in the liquid-like sc-CO_2 region, while the absolute level of swelling is higher in the liquid-like sc-CO_2 region illustrated by the higher slopes of the N_2 permeability curves.

Horn and Paul [54] showed that for relatively short (~4 h) CO_2 conditioning times at 32 atm thick Matrimid films have lower relaxation rates compared to thin films. However, the thick Matrimid films show almost complete relaxation back to the original N_2 permeability after 200 h. In our case much longer CO_2 conditioning times (~75 h) and higher CO_2 pressures (20–120 bar) are applied, resulting in a higher degree of plasticization of the films. This strong plasticization is also reflected in the considerably longer relaxation times required for the film to return to its original N_2 permeability. As mentioned before, in fact the membrane films do not return to their initial state within the time period of the experiment. From extrapolation of the N_2 permeability curves it is estimated that relaxation times longer than 1000 h (depending on CO_2 conditioning pressure) are necessary for the films to return to their initial state.

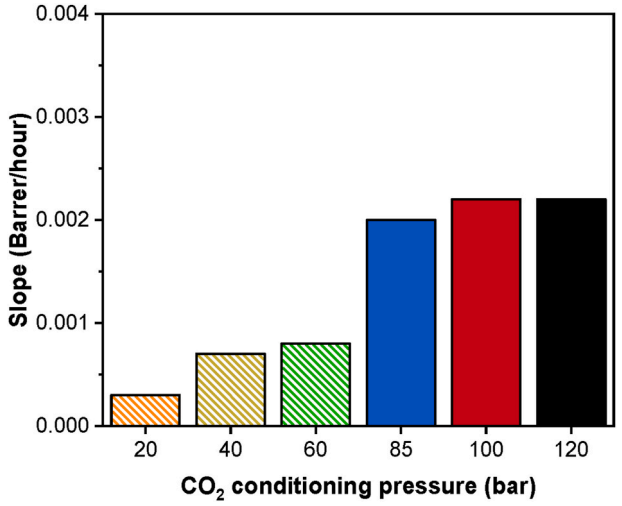

Fig. 10. Slopes of the N_2 permeability decay curves after different CO_2 conditioning pressures for Matrimid membranes at 35 °C. The slopes of the N_2 permeability curves are calculated in the experimental time interval 50–75 h. The patterned bars represent the conditioning of the membrane in the gaseous CO_2 phase whereas the solid bars represent conditioning of the membrane in the liquid-like sc-CO_2 phase.

3.4. Hysteresis and permeation history

Plasticization phenomena are commonly paired with hysteresis effects upon pressurization and depressurization steps in permeation or sorption measurements [44,55–57]. Significantly higher permeabilities and concentrations are measured when the pressure is decreased stepwise after the membrane is exposed to high pressure CO_2. Decreasing the pressure leaves extra free volume in the polymer matrix, and as shown with the N_2 permeability decay measurements the polymer chains are unable to relax back to their initial state within the measured time interval resulting in permanent network dilation [48]. Consequently, the permeation history of the polymer membrane has a large influence on the network morphology and thus on the measured CO_2 permeabilities. Fig. 11 displays hysteresis effects in the time-dependent CO_2 permeability as a function of the experimental time during pressurization, depressurization and repressurization. When initially increasing the feed pressure in the gaseous CO_2 region (20, 40 and 60 bar), a stepwise increase in CO_2 permeability is observed, similarly as observed in literature [54]. Increasing the pressure results in a greater elevation of the CO_2 permeability, due to the higher swelling of the membrane as also observed in Fig. 6. When changing the pressure into the liquid-like sc-CO_2 region the CO_2 permeability is only dependent on time and no longer on the feed pressure, as can be seen by the disappearance of the stepwise behavior. No difference in behavior is observed when either increasing or decreasing the pressure in the liquid-like sc-CO_2 region. This is expected as the CO_2 concentration remains relatively constant and no hysteresis was observed in the liquid-like sc-CO_2 region (Fig. 4). This confirms that the extent of plasticization is independent of the feed pressure in the liquid-like sc-CO_2 region. When the pressure is decreased further, the phase transition to gaseous CO_2 occurs. A reduction in CO_2 permeability is expected, because in the gaseous CO_2 region the CO_2 concentration starts to decrease and relaxation of the polymer matrix sets in. However, upon reducing the feed pressure to 60 and 40 bar, the CO_2 permeability even slightly increases and only decreases marginally over time due to relaxation of the polymer matrix. This shows that at these pressures in the gaseous CO_2 region the swelling stresses in the polymer matrix are still large enough to keep the swollen morphology of the polymer matrix intact, even though the CO_2 concentration decreases (Fig. 4). Only when decreasing the feed pressure further to 20 bar in the gaseous region considerable chain relaxation occurs, illustrated by the larger decrease in CO_2 permeability. This considerable chain relaxation at 20 bar is also represented by the lower CO_2 permeability when increasing the pressure again during the repressurization cycle. During this repressurization cycle the CO_2 permeability only increases slightly over time as the membrane is still highly plasticized from the pressurization and depressurization cycles.

In contrast to the permeation behavior during the pressurization cycle, the gaseous CO_2-liquid-like sc-CO_2 phase transition is not well visible in the permeation behavior during the depressurization and repressurization cycle (Fig. 12). As mentioned before in the liquid-like sc-CO_2 region the CO_2 permeability has no pressure dependency, but solely increases over time. This is also observed in Fig. 12 as the CO_2 permeability increases with consecutive pressure steps in the liquid-like

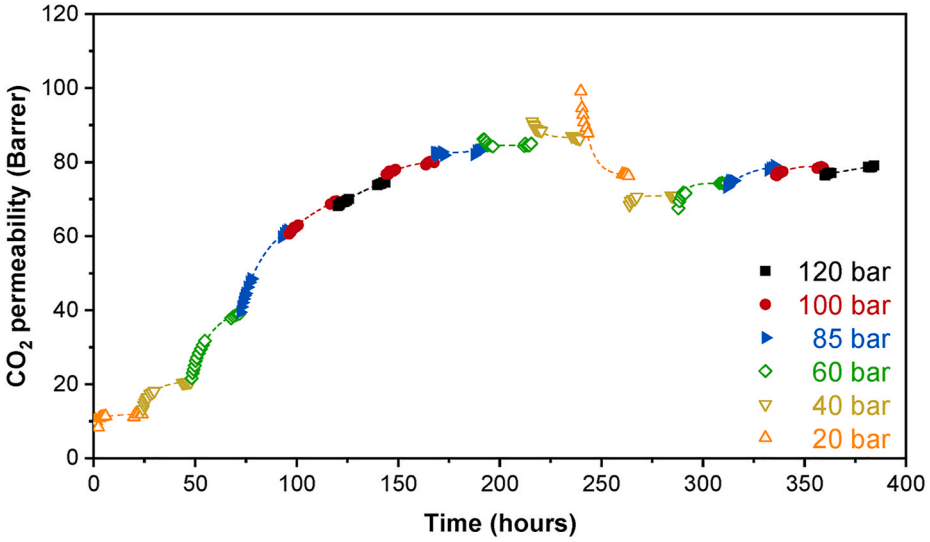

Fig. 11. Pressurization, depressurization and repressurization cycle showing hysteresis in the time-dependent CO_2 permeability (based on CO_2 fugacity) of Matrimid at 35 °C as a function of the CO_2 conditioning time. During the pressurization cycle the pressure was gradually increased from 20 to 120 bar with a time interval of 24 h at each pressure stage. Subsequently, after the final pressure was reached the pressure was gradually decreased back to 20 bar using the same time interval of 24 h. The protocol for the repressurization cycle was identical as for the pressurization cycle.

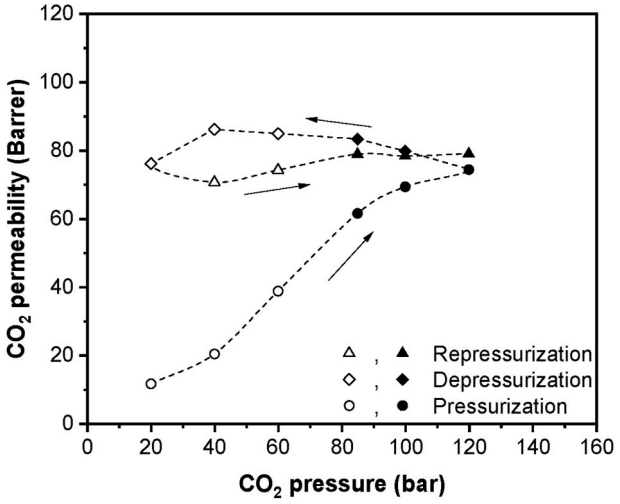

Fig. 12. Hysteresis in CO_2 permeability (based on CO_2 fugacity) of Matrimid at 35 °C as a function of the CO_2 conditioning pressure. Permeability values are taken after 24 h of conditioning at the corresponding pressure. The open symbols represent the gaseous CO_2 phase whereas the closed symbols represent the liquid-like sc-CO_2 phase.

sc-CO_2 region, independent whether the pressure is increasing or decreasing. After exposure to liquid-like sc-CO_2 the membrane is highly plasticized. The swelling stresses in the gaseous CO_2 region are sufficiently large to keep the membrane in this plasticized state and the chain relaxations slow. This results in a relatively constant CO_2 permeability as a function of pressure after exposure to liquid-like sc-CO_2. Just at a feed pressure of 20 bar, the swelling stresses are small enough for significant chain relaxation to occur, indicated by a decrease in permeability. Even at this relatively low pressure the CO_2 permeability does not decrease enormously over 24 h, showing that the chain relaxations are still relatively slow. Thus, exposing the membrane to liquid-like sc-CO_2 significantly changes the membrane morphology and affects the permeation behavior at all subsequent feed pressures.

To study the influence of the permeation history of the membrane, membranes were exposed to CO_2 for different conditioning times (Fig. 3). Fig. 13 shows the comparison of the CO_2 permeability for membrane films with different permeation histories. At 20 bar no difference between the two permeabilities could be observed as this is the first pressure step and there is no prior permeation history. When the pressure increases the influence of the permeation history becomes more pronounced. The swelling stresses at lower pressures are smaller than at higher pressures [2,6]. Therefore, increasing the feed pressure using the different conditioning times yields a different morphological state of the polymer matrix. When using only 1 h of conditioning time at preceding pressures, the pressure and thus also the CO_2 concentration increases relatively fast. Hence, the polymer matrix experiences large swelling stresses immediately. This results in higher swelling rate and thus a more

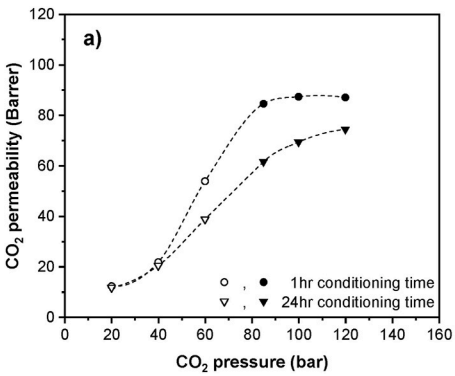

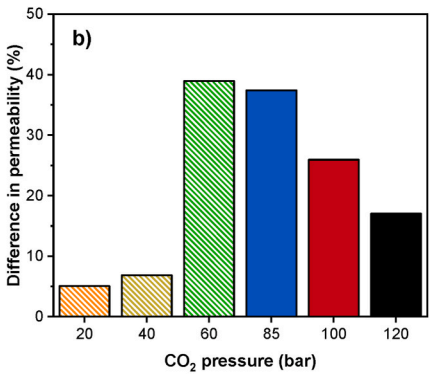

Fig. 13. a) Comparison of the CO_2 permeability (based on CO_2 fugacity) of Matrimid at 35 °C as a function of pressure for different conditioning times at preceding pressures. All permeability values are taken after 24 h of permeation at the respective pressure. The open symbols represent the gaseous CO_2 phase whereas the closed symbols represent the liquid-like sc-CO_2 phase. **b)** Relative difference in permeability values at the respective pressures between the membrane films with 1hr and 24hr conditioning time. The patterned bars represent the conditioning of the membrane in the gaseous CO_2 phase whereas the solid bars represent conditioning of the membrane in the liquid-like sc-CO_2 phase.

swollen morphology, as shown by the higher permeabilities for the membranes that have 1 h of conditioning time. Even though the membranes that have a 24 h conditioning time have been exposed to CO_2 above the plasticization pressure for considerably longer times, the membranes are more swollen at shorter conditioning times. Reasons for this are found in the relaxation history of the polymer matrix [6,58]. When the polymer matrix is exposed to small swelling stresses at low pressures for 24 h, the swelling of the polymer matrix occurs gradually, and the polymer chains have more time to reorient. Thus, at a subsequent pressure step, the polymer matrix is not subjected to huge differences in swelling stresses. This results in less swollen membranes when longer CO_2 conditioning times are applied. The difference in CO_2 permeability for the different conditioning times becomes smaller after the transition to liquid-like sc-CO_2. Given that the swelling stress is constant in the liquid-like sc-CO_2 region, the extent of plasticization is independent of the feed pressure and solely increases over time. Therefore, this smaller difference in CO_2 permeability for the different conditioning times is attributed to the different total exposure time to liquid-like sc-CO_2. The CO_2 permeability of the membranes with 1 h of conditioning time barely increases in the liquid-like sc-CO_2 region. This is because the total exposure time to liquid-like sc-CO_2 is much lower when a 1 h conditioning time is applied compared to when 24 h conditioning time is applied at preceding pressures (Fig. 3). Hence, the total exposure time to the same swelling stress is different, which results in the smaller difference in CO_2 permeability with increasing pressure for the different conditioning times. However, it is expected that when the membranes are exposed to liquid-like sc-CO_2 for longer time the differences in morphological state of the polymer between the conditioning times will decrease, as the swelling over time will decrease and hypothetically ultimately stops.

4. Conclusions

The time-dependent CO_2-induced plasticization behavior at supercritical conditions of glassy Matrimid polymer membranes has been extensively investigated by conditioning the polyimide membranes with both gaseous CO_2 and liquid-like sc-CO_2. The membranes were evaluated for their time-dependent gas sorption and permeation at CO_2 pressures ranging from 20 to 120 bar. In the gaseous CO_2 region, the CO_2 sorption could be well described using the dual mode sorption model, while in the liquid-like sc-CO_2 region the CO_2 sorption was directly dependent on the CO_2 density. In the liquid-like sc-CO_2 region the CO_2 concentration remained constant as a function of time and showed no hysteresis, which was attributed to a glass transition that is induced by the high CO_2 sorption. The CO_2 permeability on the other hand, showed more pronounced time-dependent behavior with increasing feed pressure as a result of polymer membrane plasticization and the increasing CO_2 density. In the liquid-like sc-CO_2 region the CO_2 permeability, and thus the extent of plasticization, was found to be independent of the feed pressure, but still showed a strong time-dependency. The difference between the observed time-dependent behavior during sorption and permeation experiments is proposed to be caused by the presence of a concentration gradient in the permeation experiments. Thus, during permeation the CO_2 concentration will not be high enough to surpass the glass transition temperature over the entire thickness of the membrane. N_2 permeability decay measurements revealed severe permanent network dilation and low polymer chain relaxation rates after exposure to liquid-like sc-CO_2. The relaxation rate of the polymer chains is related to the level of swelling in the polymer, where a higher swelling degree resulted in a higher initial relaxation rate. The membranes showed strong hysteresis effects. Exposure to liquid-like sc-CO_2 resulted in a highly plasticized membrane and changed the permeation behavior at all subsequent feed pressures. Moreover, the permeation history of the membrane had a large influence on the plasticization effects, as shorter conditioning times resulted in more swollen membranes compared to longer conditioning times at preceding pressures.

CRediT authorship contribution statement

Menno Houben: Conceptualization, Methodology, Validation, Formal analysis, Investigation, Writing – Original Draft, Writing – Review & Editing, Visualization. **Machiel van Essen:** Formal analysis, Investigation, Writing - review & editing. **Kitty Nijmeijer:** Conceptualization, Supervision, Writing - review & editing, Project administration, Funding acquisition. **Zandrie Borneman:** Conceptualization, Supervision, Writing - review & editing.

Declaration of competing interest

The authors declare that they have no known competing financial interests or personal relationships that could have appeared to influence the work reported in this paper.

Acknowledgements

This research did not receive any specific grant from funding agencies in the public, commercial, or not-for-profit sectors. The authors wish to express their gratitude to Wetsus, Centre of Excellence for Sustainable Water Technology, for providing the high-pressure permeation equipment.

References

[1] A. Bos, I.G.M. Pünt, M. Wessling, H. Strathmann, CO_2-induced plasticization phenomena in glassy polymers, J. Membr. Sci. 155 (1999) 67–78, https://doi.org/10.1016/S0376-7388(98)00299-3.
[2] M. Wessling, S. Schoeman, T. van der Boomgaard, C.A. Smolders, Plasticization of gas separation membranes, Gas Separ. Purif. 5 (1991) 222–228, https://doi.org/10.1016/0950-4214(91)80028-4.
[3] M. Houben, Z. Borneman, K. Nijmeijer, Plasticization behavior of crown-ether containing polyimide membranes for the separation of CO_2, Separ. Purif. Technol. 255 (2021), 117307, https://doi.org/10.1016/j.seppur.2020.117307.
[4] J.D. Wind, S.M. Sirard, D.R. Paul, P.F. Green, K.P. Johnston, W.J. Koros, Carbon dioxide-induced plasticization of polyimide membranes: pseudo-equilibrium relationships of diffusion, sorption, and swelling, Macromolecules 36 (2003) 6433–6441, https://doi.org/10.1021/ma0343582.
[5] J.D. Wind, C. Staudt-Bickel, D.R. Paul, W.J. Koros, The effects of crosslinking chemistry on CO_2 plasticization of polyimide gas separation membranes, Ind. Eng. Chem. Res. 41 (2002) 6139–6148, https://doi.org/10.1021/ie0204639.
[6] M. Wessling, I. Huisman, T. van der Boomgaard, C.A. Smolders, Time-dependent permeation of carbon dioxide through a polyimide membrane above the plasticization pressure, J. Appl. Polym. Sci. 58 (1995) 1959–1966, https://doi.org/10.1002/app.1995.070581105.
[7] A. Bos, I.G.M. Pünt, M. Wessling, H. Strathmann, Plasticization-resistant glassy polyimide membranes for CO_2/CH_4 separations, Separ. Purif. Technol. 14 (1998) 27–39, https://doi.org/10.1016/S1383-5866(98)00057-4.
[8] A. Bos, I. Pünt, H. Strathmann, M. Wessling, Suppression of gas separation membrane plasticization by homogeneous polymer blending, AIChE J. 47 (2001) 1088–1093, https://doi.org/10.1002/aic.690470515.
[9] S. Shahid, K. Nijmeijer, Performance and plasticization behavior of polymer-MOF membranes for gas separation at elevated pressures, J. Membr. Sci. 470 (2014) 166–177, https://doi.org/10.1016/j.memsci.2014.07.034.
[10] S.R. Reijerkerk, K. Nijmeijer, C.P. Ribeiro, B.D. Freeman, M. Wessling, On the effects of plasticization in CO_2/light gas separation using polymeric solubility selective membranes, J. Membr. Sci. 367 (2011) 33–44, https://doi.org/10.1016/j.memsci.2010.10.035.
[11] Thermophysical Properties of Fluid Systems - NIST, National Institute of Standards and Technology, 2016. http://webbook.nist.gov/chemistry/fluid/. (Accessed 5 April 2017). accessed.
[12] M. Houben, R. van Geijn, M. van Essen, Z. Borneman, K. Nijmeijer, Supercritical CO_2 permeation in glassy polyimide membranes, J. Membr. Sci. 620 (2021) 118922, https://doi.org/10.1016/j.memsci.2020.118922.
[13] A.M. Kratochvil, S. Damle-Mogri, W.J. Koros, Effects of supercritical CO_2 conditioning on un-cross-linked polyimide membranes for natural gas purification, Macromolecules 42 (2009) 5670–5675, https://doi.org/10.1021/ma900853j.
[14] A. Shamu, H. Miedema, S.J. Metz, Z. Borneman, K. Nijmeijer, Mass transfer studies on the dehydration of supercritical carbon dioxide using dense polymeric membranes, Separ. Purif. Technol. 209 (2019) 229–237, https://doi.org/10.1016/j.seppur.2018.07.042.
[15] T. Lohaus, M. Scholz, B.T. Koziara, N.E. Benes, M. Wessling, Drying of supercritical carbon dioxide with membrane processes, J. Supercrit. Fluids 98 (2015) 137–146, https://doi.org/10.1016/j.supflu.2015.01.009.
[16] S. Sarrade, C. Guizard, G.M. Rios, New applications of supercritical fluids and supercritical fluids processes in separation, Separ. Purif. Technol. 32 (2003) 57–63, https://doi.org/10.1016/S1383-5866(03)00054-6.

[17] M. Mazzotti, R. Pini, G. Storti, Enhanced coalbed methane recovery, J. Supercrit. Fluids 47 (2009) 619–627, https://doi.org/10.1016/j.supflu.2008.08.013.
[18] A. Shamu, M. Dunnewold, H. Miedema, Z. Borneman, K. Nijmeijer, Permeation of supercritical CO_2 through dense polymeric membranes, J. Supercrit. Fluids 144 (2019) 63–70, https://doi.org/10.1016/j.supflu.2018.10.009.
[19] G.G. Simeoni, T. Bryk, F.A. Gorelli, M. Krisch, G. Ruocco, M. Santoro, T. Scopigno, The Widom line as the crossover between liquid-like and gas-like behaviour in supercritical fluids, Nat. Phys. 6 (2010) 503–507, https://doi.org/10.1038/nphys1683.
[20] A.R. Imre, C. Ramboz, U.K. Deiters, T. Kraska, Anomalous fluid properties of carbon dioxide in the supercritical region: application to geological CO_2 storage and related hazards, Environ. Earth Sci. 73 (2015) 4373–4384, https://doi.org/10.1007/s12665-014-3716-5.
[21] J.D. Wind, S.M. Sirard, D.R. Paul, P.F. Green, K.P. Johnston, W.J. Koros, Relaxation dynamics of CO_2 diffusion, sorption, and polymer swelling for plasticized polyimide membranes, Macromolecules 36 (2003) 6442–6448, https://doi.org/10.1021/ma034359u.
[22] S. Kanehashi, T. Nakagawa, K. Nagai, X. Duthie, S. Kentish, G. Stevens, Effects of carbon dioxide-induced plasticization on the gas transport properties of glassy polyimide membranes, J. Membr. Sci. 298 (2007) 147–155, https://doi.org/10.1016/j.memsci.2007.04.012.
[23] G. Soave, M. Barolo, A. Bertucco, Estimation of high-pressure fugacity coefficients of pure gaseous fluids by a modified SRK equation of state, Fluid Phase Equil. 91 (1993) 87–100, https://doi.org/10.1016/0378-3812(93)85081-V.
[24] C.A. Scholes, W.X. Tao, G.W. Stevens, S.E. Kentish, Sorption of methane, nitrogen, carbon dioxide, and water in Matrimid 5218, J. Appl. Polym. Sci. 117 (2010) 2284–2289, https://doi.org/10.1002/app.32148.
[25] V. Stannett, The transport of gases in synthetic polymeric membranes-an historic perspective, J. Membr. Sci. 3 (1978) 97–115, https://doi.org/10.1016/S0376-7388(00)83016-1.
[26] A.J. Erb, D.R. Paul, Gas sorption and transport in polysulfone, J. Membr. Sci. 8 (1981) 11–22, https://doi.org/10.1016/S0376-7388(00)82135-3.
[27] W.R. Vieth, J.M. Howell, J.H. Hsieh, Dual sorption theory, J. Membr. Sci. 1 (1976) 177–220, https://doi.org/10.1016/S0376-7388(00)82267-X.
[28] S. Kanehashi, K. Nagai, Analysis of dual-mode model parameters for gas sorption in glassy polymers, J. Membr. Sci. 253 (2005) 117–138, https://doi.org/10.1016/j.memsci.2005.01.003.
[29] S.P. Nalawade, F. Picchioni, L.P.B.M. Janssen, V.E. Patil, J.T.F. Keurentjes, R. Staudt, Solubilities of sub- and supercritical carbon dioxide in polyester resins, Polym. Eng. Sci. 46 (2006) 643–649, https://doi.org/10.1002/pen.
[30] M. Minelli, G.C. Sarti, Gas transport in glassy polymers: prediction of diffusional time lag, Membranes 8 (2018) 1–15, https://doi.org/10.3390/membranes8010008.
[31] L. Wang, J.P. Corriou, C. Castel, E. Favre, Transport of gases in glassy polymers under transient conditions: limit-behavior investigations of dual-mode sorption theory, Ind. Eng. Chem. Res. 52 (2013) 1089–1101, https://doi.org/10.1021/ie2027102.
[32] J. Von Schnitzler, R. Eggers, Mass transfer in polymers in a supercritical CO_2-atmosphere, J. Supercrit. Fluids 16 (1999) 81–92, https://doi.org/10.1016/S0896-8446(99)00020-0.
[33] M. Askari, CO_2/CH_4 sorption behavior of glassy polymeric membranes based on dual mode sorption model, Bull. La Société R. Des Sci. Liège. 86 (2017) 139–156.
[34] T. Chung, S.S. Chan, R. Wang, Z. Lu, C. He, Characterization of permeability and sorption in Matrimid/C60 mixed matrix membranes, J. Membr. Sci. 211 (2003) 91–99, https://doi.org/10.1016/S0376-7388(02)00385-X.
[35] S.M. Sirard, K.J. Ziegler, I.C. Sanchez, P.F. Green, K.P. Johnston, Anomalous properties of poly(methyl methacrylate) thin films in supercritical carbon dioxide, Macromolecules 35 (2002) 1928–1935, https://doi.org/10.1021/ma011384w.
[36] W.-C.V. Wang, E.J. Kramer, W.H. Sachse, Effects of high-pressure CO_2 on the glass transition temperature and mechanical properties of polystyrene, J. Polym. Sci. 2 Polym. Phys. 20 (1982) 1371–1384, https://doi.org/10.1002/pol.1982.180200804.
[37] B. Krause, R. Mettinkhof, N.F.A. Van Der Vegt, M. Wessling, Microcellular foaming of amorphous high-Tg polymers using carbon dioxide, Macromolecules 34 (2001) 874–884, https://doi.org/10.1021/ma001291z.
[38] M. Wessling, Z. Borneman, T. van den Boomgaard, C.A. Smolders, Carbon dioxide foaming of glassy polymers, J. Appl. Polym. Sci. 53 (1994) 1497–1512.
[39] J.S. Vrentas, C.M. Vrentas, Sorption in glassy polymers, Macromolecules 24 (1991) 2404–2412, https://doi.org/10.1021/ma00009a043.
[40] T.S. Chow, Molecular interpretation of the glass transition temperature of polymer-diluent systems, Macromolecules 364 (1980) 362–364.
[41] B. Krause, H.J.P. Sijbesma, P. Mu, Bicontinuous nanoporous polymers by carbon dioxide foaming, Macromolecules 34 (2001) 8792–8801, https://doi.org/10.1021/ma010854j.
[42] T. Visser, M. Wessling, When do sorption-induced relaxations in glassy polymers set in? Macromolecules 40 (2007) 4992–5000, https://doi.org/10.1021/ma070202g.
[43] M. Minelli, G.C. Sarti, Permeability and diffusivity of CO_2 in glassy polymers with and without plasticization, J. Membr. Sci. 435 (2013) 176–185, https://doi.org/10.1016/j.memsci.2013.02.013.
[44] K. Simons, K. Nijmeijer, J.G. Sala, H. van der Werf, N.E. Benes, T.J. Dingemans, M. Wessling, CO_2 sorption and transport behavior of ODPA-based polyetherimide polymer films, Polymer 51 (2010) 3907–3917, https://doi.org/10.1016/j.polymer.2010.06.031.
[45] J. Potreck, K. Nijmeijer, T. Kosinski, M. Wessling, Mixed water vapor/gas transport through the rubbery polymer PEBAX® 1074, J. Membr. Sci. 338 (2009) 11–16, https://doi.org/10.1016/j.memsci.2009.03.051.
[46] J.C. Legros, A. Mialdun, P. Strizhak, V. Shevtsova, Permeation of supercritical CO_2 through perfluoroelastomers, J. Supercrit. Fluids 126 (2017) 1–13, https://doi.org/10.1016/j.supflu.2017.02.022.
[47] V.E. Patil, L.J.P. Van Den Broeke, F.F. Vercauteren, J.T.F. Keurentjes, Permeation of supercritical carbon dioxide through polymeric hollow fiber membranes, J. Membr. Sci. 271 (2006) 77–85, https://doi.org/10.1016/j.memsci.2005.06.059.
[48] T. Visser, G.H. Koops, M. Wessling, On the subtle balance between competitive sorption and plasticization effects in asymmetric hollow fiber gas separation membranes, J. Membr. Sci. 252 (2005) 265–277, https://doi.org/10.1016/j.memsci.2004.12.015.
[49] T. Visser, N. Masetto, M. Wessling, Materials dependence of mixed gas plasticization behavior in asymmetric membranes, J. Membr. Sci. 306 (2007) 16–28, https://doi.org/10.1016/j.memsci.2007.07.048.
[50] B.W. Rowe, B.D. Freeman, D.R. Paul, Physical aging of ultrathin glassy polymer films tracked by gas permeability, Polymer 50 (2009) 5565–5575, https://doi.org/10.1016/j.polymer.2009.09.037.
[51] D. Punsalan, W.J. Koros, Drifts in penetrant partial molar volumes in glassy polymers due to physical aging, Polymer 46 (2005) 10214–10220, https://doi.org/10.1016/j.polymer.2005.06.061.
[52] N. Müller, U.A. Handge, V. Abetz, Physical ageing and lifetime prediction of polymer membranes for gas separation processes, J. Membr. Sci. 516 (2016) 33–46, https://doi.org/10.1016/j.memsci.2016.05.055.
[53] Y. Huang, D.R. Paul, Effect of film thickness on the gas-permeation characteristics of glassy polymer membranes, Ind. Eng. Chem. Res. 46 (2007) 2342–2347, https://doi.org/10.1021/ie0610804.
[54] N.R. Horn, D.R. Paul, Carbon dioxide plasticization and conditioning effects in thick vs. thin glassy polymer films, Polymer 52 (2011) 1619–1627, https://doi.org/10.1016/j.polymer.2011.02.007.
[55] Z.P. Smith, G. Hernández, K.L. Gleason, A. Anand, C.M. Doherty, K. Konstas, C. Alvarez, A.J. Hill, A.E. Lozano, D.R. Paul, B.D. Freeman, Effect of polymer structure on gas transport properties of selected aromatic polyimides, polyamides and TR polymers, J. Membr. Sci. 493 (2015) 766–781, https://doi.org/10.1016/j.memsci.2015.06.032.
[56] A.C. Puleo, D.R. Paul, The effect of degree of acetylation on gas sorption and transport behavior in cellulose acetate, J. Membr. Sci. 47 (1989) 301–332, https://doi.org/10.1016/S0376-7388(00)83083-5.
[57] W.R. Vieth, L.H. Dao, H. Pedersen, Non-equilibrium microstructural and transport characteristics of glassy poly (ethylene terephthalate), J. Membr. Sci. 60 (1991) 41–62, https://doi.org/10.1016/S0376-7388(00)80323-3.
[58] J.S. Chiou, D.R. Paul, Effects of CO_2 exposure on gas transport properties of glassy polymers, J. Membr. Sci. 32 (1987) 195–205, https://doi.org/10.1016/S0376-7388(00)85006-1.